Eur. Phys. J. Special Topics **225**, 2613–2622 (2016)

DOI: 10.1140/epjst/e2016-60012-4

THE EUROPEAN PHYSICAL JOURNAL SPECIAL TOPICS

Regular Article

Phase locked periodic solutions and synchronous chaos in a model of two coupled molecular lasers

Eusebius J. Doedel[1,a], and Carlos L. Pando Lambruschini[2,b]

[1] Department of Computer Science, Concordia University, 1455 boulevard de Maisonneuve O., Montréal, Québec H3G 1M8, Canada
[2] Instituto de Física, Benemérita Universidad Autónoma de Puebla, Apdo. Postal J-48, Puebla, Puebla 72570, México

Received 23 January 2016 / Received in final form 28 June 2016
Published online 22 November 2016

Abstract. We study a rate-equation model for two coupled molecular lasers with a saturable absorber. A numerical bifurcation study shows the existence of isolas for in-phase periodic solutions as physical parameters change. In addition there are other non-isola families of in-phase, anti-phase and intermediate-phase periodic oscillations. In this model the unstable periodic orbits belonging to the in-phase isolas constitute a skeleton of the attractor, when chaotic synchronization sets in for a set of physically relevant control parameters.

1 Introduction

In this study we consider the dynamics of a coupled optical system which can exhibit complex mixed mode oscillations. Mixed mode oscillations (MMO) display multiple time scales and are currently the subject of substantial research, because MMO are ubiquitous in nature and have been observed for several decades in different chemical, physical, biological, and engineering experimental systems [1–6]. Quantum optical systems may also display multiple time scales within the semiclassical description. In particular, laser devices in the Q-switching operation typically emit short and intense pulses of light that are followed by time intervals with minimal laser intensity [7–9]. In this type of lasers, a saturable absorber or an electro-optical element allows the energy inside the system to be accumulated and stored long enough before it is suddenly released as an optical pulse. Q-switching operation is a general phenomenon, and has been achieved in many types of laser gain media, such as in semiconductors and optical fibers [10,11], where the pulse durations are of the order of microseconds, nanoseconds and even picoseconds in gas, semiconductor and microchip lasers, respectively [8].

There are several optical coupling schemes, where phenomena related to phase locking and chaotic synchronization are important issues [8]. In this article we consider a special type of optical coupling for Q-switched lasers, namely, coupling via

[a] e-mail: doedel@cs.concordia.ca
[b] e-mail: carlos@ifuap.buap.mx

saturable absorbers. This coupling mechanism has been studied theoretically and experimentally for CO_2 lasers [12–14], where one of the main goals was precisely to achieve optical chaotic synchronization. One of the features of this form of nonlinear coupling between two lasers is that the resulting model provides an interesting analogy with the field of neuroscience. The corresponding neuronal systems are pairs of reciprocally inhibiting neurons, known as half-center oscillators; they typically display behaviors characterized by anti-phase bursting, and are the building blocks of central pattern generators that produce various phase-locked bursting rhythms [15,16].

In this article we show that a model for two absorber-coupled Q-switched CO_2 lasers predicts that there are isolas of in-phase periodic solutions. This model also shows characteristic families of in-phase and anti-phase periodic solutions, which arise from Hopf bifurcations along families of stationary solutions. Periodic solutions with a fixed intermediate-phase difference, also known as phase-locked solutions, arise from subsequent symmetry-breaking bifurcations. In our model the unstable periodic orbits (UPO) that arise from the in-phase isolas constitute the skeleton of the attractor when chaotic synchronization sets in, for a set of physically relevant control parameters. It is worthwhile mentioning that these isolas do not exist in the basic rate-equation model [17]. Our solutions are complemented by two-parameter bifurcation diagrams in the plane of the pump current and coupling strength, as obtained by a numerical continuation study with the package AUTO [18]. In Sect. 2 we introduce and discuss the model, and in Sect. 3 we present its bifurcation analysis and numerical simulations; conclusions and a discussion are presented in Sect. 4.

2 A model for two coupled single-mode molecular lasers

We study the effects of moderate and mutual coupling in class-B single-mode Q-switched lasers: a symmetric pair of CO_2 lasers with a saturable absorber (LSA). Each of these uncoupled laser devices is described by a model known as the four-level model [19,20]. The CO_2 LSA is an important example of class-B lasers and its giant laser spikes are known as passive Q-switching (PQS) self-pulsations. The complex instabilities found in this system gave rise to early studies in nonlinear dynamics about three decades ago [7,9,21–24]. As a result the rich dynamical phenomenology of the CO_2 LSA made it an interesting object for study in nonlinear dynamics [25–33].

We consider the dynamical effects caused by a special type of optical coupling of Q-switched lasers, namely coupling via saturable absorbers, which is also a form of incoherent coupling. This coupling mechanism between laser devices has been implemented theoretically and experimentally in previous studies of CO_2 lasers [12–14]. The coupling is based on the injection of the electric field of one laser device into the absorber of the symmetric device, such that the laser modes (field polarizations) are not injected into the symmetric cavity. This partially saturates the transition levels of the symmetric absorber, which in turn couples the lasers.

Under suitable approximations [19,20] each of the two laser devices is described by a reduced four-level model and can be coupled via fast saturable absorbers. This system is modeled in Eq. (1), where I_i stands for the field intensities within the laser cavities, the fast variables, and v_i and w_i denote the effective populations of the lower and upper (excited) rotational energy levels in the gain medium, respectively, $i = 1, 2$. v_i and w_i are the slow variables. Q is the incoherent pump induced by the excitation current in the gain medium, and z is the effective number of reservoir rotational levels in each vibrational band in the gain medium. The last term in the equations for I_i stands for the saturable absorber, the parameter α is proportional to the density of absorber molecules and β is known as the saturability [19,20]. c stands for the coupling parameter via fast saturable absorbers. The vibrational relaxation rates for

the upper (excited) and lower vibrational levels in the CO_2 molecules are called γ_2 and γ_1, respectively. The relaxation constants γ_i have been suitably normalized in Eq. (1).

$$\begin{aligned}
\frac{dI_1}{dt} &= I_1\Big(-1+\frac{(z+1)\Omega_1}{z}(w_1-v_1)-\frac{\alpha}{1+2\beta(I_1+cI_2)}\Big)\ ,\\
\frac{dv_1}{dt} &= \Omega_1 I_1(w_1-v_1)-\gamma_1 v_1\ ,\\
\frac{dw_1}{dt} &= \Omega_1 I_1(v_1-w_1)-\gamma_2 w_1+z\gamma_2 Q\ ,\\
\frac{dI_2}{dt} &= I_2\Big(-1+\frac{(z+1)\Omega_2}{z}(w_2-v_2)-\frac{\alpha}{1+2\beta(I_2+cI_1)}\Big)\ ,\\
\frac{dv_2}{dt} &= \Omega_2 I_2(w_2-v_2)-\gamma_1 v_2\ ,\\
\frac{dw_2}{dt} &= \Omega_2 I_2(v_2-w_2)-\gamma_2 w_2+z\gamma_2 Q\ .
\end{aligned} \tag{1}$$

Also in Eq. (1), we have defined

$$\Omega_i=\frac{z+1}{(z+1)^2+2zI_i/\gamma_{R'}}\ ,\quad i=1,2,$$

where $\gamma_R^{'}$ stands for the characteristic rotational relaxation rates of CO_2 molecules within the same vibrational band [19,20].

Physical processes similar to those that take place in the active medium may also occur in the saturable absorber of a gas cell, but the absorber may also have a different nature, such as in semiconductor saturable absorbers (SESAM) devices [10]. In our model we assume that a fast saturable absorber is described by a two level model with fast relaxation rates.

For numerical purposes it is useful to rewrite the equations for I_1 and I_2 in terms of $\log(I_1)$ and $\log(I_2)$. The fixed parameter values are $\alpha=0.75$, $\gamma_R'=0.2205$, $\gamma_1=0.0252$, $\gamma_2=0.00315$, $z=10$, and $\beta=200$, while Q and the coupling strength c are used as continuation parameters. When $c=0$, Eq. (1) decouples into two independent sets of three equations. When c is nonzero, the synchronous (or in-phase) solutions, *i.e.*, solutions with $I_1(t)=I_2(t)=I(t)$, $v_1(t)=v_2(t)=v(t)$, and $w_1(t)=w_2(t)=w(t)$, satisfy

$$\begin{aligned}
\frac{dI}{dt} &= I\Big(-1+\frac{(z+1)\Omega}{z}(w-v)-\frac{\alpha}{1+2\beta(1+c)I}\Big)\ ,\\
\frac{dv}{dt} &= \Omega I(w-v)-\gamma_1 v\ ,\\
\frac{dw}{dt} &= \Omega I(v-w)-\gamma_2 w+z\gamma_2 Q\ ,
\end{aligned} \tag{2}$$

which is not identical to the uncoupled case. To be specific, the synchronous solution structure for given value of β in Eq. (1) corresponds to taking $\hat{\beta}(c)=\beta(1+c)$. Moreover, the stability properties of periodic solutions can be different for Eq. (1) and Eq. (2), for the same values of the coupling strengths.

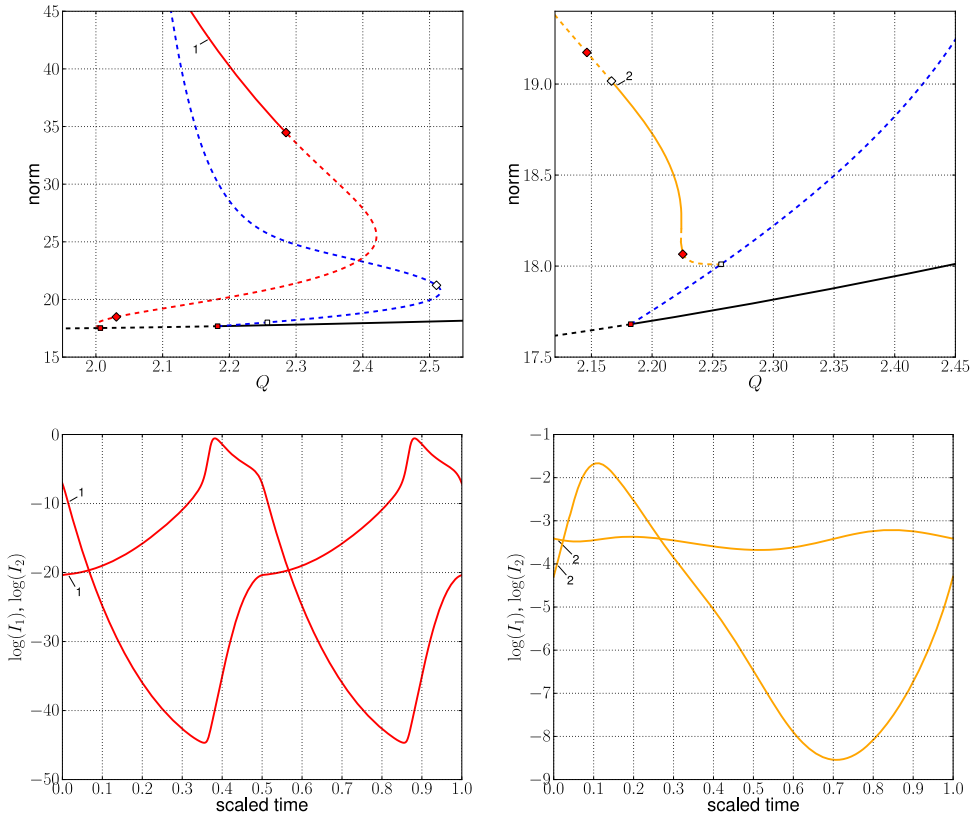

Fig. 1. Top-left: The black curve represents nonzero stationary states with two Hopf bifurcation (solid red squares), from which bifurcate a family of in-phase periodic solutions (blue) and a family of anti-phase periodic solutions (red), respectively. Top-right: A detail of the in-phase family, also showing a bifurcating intermediate-phase family (orange). Bottom: Representative solutions from the top panels. Coupling parameter $c = 0.14$.

In our case of two mutually and symetrically coupled CO_2 lasers, the geometrical configuration is similar to the case of two unidirectionally coupled CO_2 lasers [13]. Moreover, the saturable absorber is assumed to be fast and identical in both lasers.

3 Numerical bifurcation analysis and synchronization

In this section we describe the solution structure of Eq. (1). We do this for a moderate value of the coupling constant c, namely, $c = 0.14$. This value is large enough for stable, synchronous solutions to exist, while it is also small enough for the presence of stable asynchronous behavior. Since the solution structure is significantly more complex than that of the single laser equations [19], we will explain this structure through a sequence of diagrams, that together provide an overview of the basic solution families and their bifurcations. In our bifurcation diagrams, solid/dashed curves represent stable/unstable solutions, respectively, Hopf bifurcations are shown as solid red squares, branch points as small open squares, period-doubling bifurcations as open diamonds, and torus bifurcations as solid red diamonds.

Two bifurcation diagrams for $c = 0.14$ are shown in the top panels of Fig. 1, while the bottom panels show the actual solutions at the labeled points in the

bifurcation diagrams. The black curve in the top-left diagram represents nonzero stationary states, which are stable beyond the Hopf bifurcation (solid red square) on the right, from which bifurcates a family of synchronous periodic solutions (blue). A family of anti-phase periodic solutions (red) emanates from the Hopf bifurcation on the left. A representative anti-phase solution is shown in the bottom-left panel. The upper part of the anti-phase family (red) in Fig. 1 contains a region of stable periodic solutions (solid red curve), delimited on the right by a torus bifurcation. Along the anti-phase family the period increases as Q decreases. It is important to mention that these "stable" anti-phase orbits are only marginally stable. Due to phase invariance there is always one Floquet multiplier that is equal to 1. However, the "stable" anti-phase orbits have another Floquet multiplier that, although less than 1, is extremely close to 1, due to the fact that the two lasers in anti-phase mode become nearly uncoupled as the period increases. Along the in-phase family (blue) in Fig. 1 is a branch point (open square) that is very close to the Hopf bifurcation point, as seen more clearly in the blow-up in the top-right panel. Also shown in the top-right panel is the bifurcating family (orange) that consist of intermediate-phase solutions. A representative solution along this intermediate-phase family is shown in the bottom-right panel. The intermediate-phase family actually consists of two symmetric branches, where the symmetry consists of interchanging the two lasers. In Fig. 1 these two branches coincide, due to the fact that an integral L_2-norm is used to represent solutions on the vertical axis. Note that the intermediate-phase family contains two regions of stability (solid orange). One of the stability intervals is bordered on the left by a period-doubling bifurcation (open diamond) and on the right by a fold. (The bifurcating period-doubled family is not shown.) The other, very small stability interval is bordered on the left by a fold and on the right by a torus bifurcation (solid red diamond). Note also the coexistence of stable stationary solutions, stable anti-phase solutions, and stable intermediate-phase solutions; for example, at $Q = 2.2$.

The top-left panel of Fig. 2 again shows the in-phase (blue) family, omitting the anti-phase and the intermediate-phase families, but now indicating a bifurcating period-doubled family (brown) consisting of unstable solutions, one of which is shown in the bottom-left panel. The top-right panel of Fig. 2 shows another family of intermediate-phase solutions (orange). This family is shown together with the unstable in-phase family (blue), even though the two families are not connected in this region. The upper part of this intermediate-phase family consists of stable orbits (solid orange), delimited by a fold on the right. The stable solution with label 4 is shown in the bottom-right panel, where it can be observed that the two lasers are "almost in phase", *i.e.*, they have an almost identical output, with only a small phase shift, as is typical of the stable solutions of this family.

The top-left panel of Fig. 3 shows isolas (purple) of in-phase periodic orbits, with a blow-up in the top-right panel. For reference, the stationary family (black), the in-phase family (blue), and its period-doubled family (brown), are also shown, but the anti-phase family and the two intermediate-phase families are omitted. The isolas are like the isolas that exist in the single laser model for $\hat{\beta} = \beta(1 + c) \cong 228$. However, unlike the single laser model, the isolas now contain branch points, and correspondingly the orbits along the isolas have different stability properties compared to the single laser case. Two representative solutions are shown in the bottom panels, namely, solutions along the isolas designated as I_{03} and I_{04}. These solutions correspond to period-doubling points that border stability regions, but they look much like the stable solutions that are observed strictly inside the stability regions.

The branch points along the isolas are of pitchfork type, *i.e.*, they give rise to two symmetric branches of symmetry-related orbits, which coincide with each other in the bifurcation diagram. A few families that bifurcate from the isolas have been partially computed, namely the initial, stable portion of these families (green), as seen in the

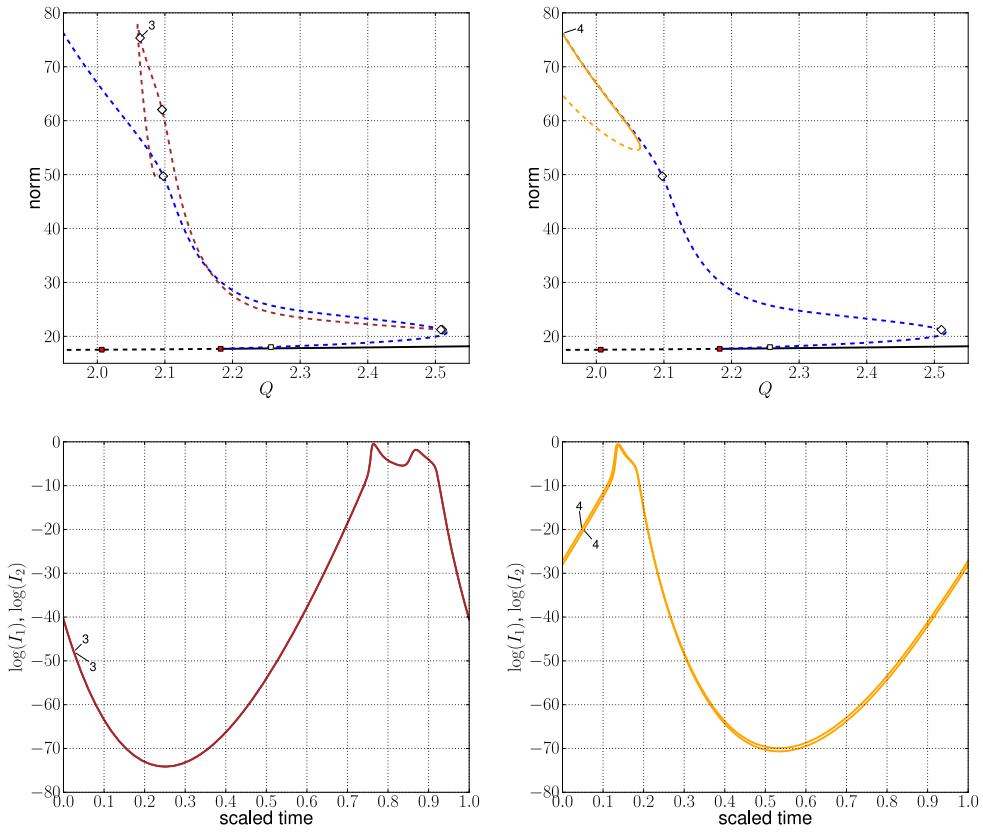

Fig. 2. Top-left: The stationary family (black) and the in-phase family (blue), also indicating a bifurcating period-doubled family (brown). Top-right: Another family of intermediate-phase solutions (orange), shown together with the stationary family (black) and the in-phase family (blue). Bottom: Representative solutions from the top panels. For the solution labeled 4, note the small phase shift between the two lasers. Coupling parameter $c = 0.14$.

top-left panel of Fig. 4. Three representative solutions, labeled 7,8, and 9, are shown in the remaining three panels. For example, the solution labeled 7 lies along the family that bifurcates from the isola I_{03}, whose periodic orbits are in-phase and have three maxima. As seen in the top-right panel of Fig. 4, the two lasers that correspond to orbit 7 have a small phase shift relative to each other. Similarly, the two orbits labeled 8 and 9, which lie along families bifurcating from I_{04} and I_{05}, respectively, display a similar phase shift. As indicated in the bifurcation diagram in Fig. 4, the solutions labeled 7,8, and 9 actually correspond to period-doubling bifurcation points where the green families become unstable. However, these solutions are representative of nearby stable solutions.

Solutions along the isolas (purple) are in-phase solutions, *i.e.*, the orbits of the two lasers are identical and have the same phase. For solutions along the green families, which bifurcate from the isolas, the individual orbits of the two lasers appear to be phase-shifted. In reality the individual orbits are not exactly the same, when each is projected to 3D space. The green families continue to exist beyond the small portions shown in Fig. 4, and they give rise to a very complex solution structure that will be investigated in a future study. Figure 5 shows loci of folds, branch points, and

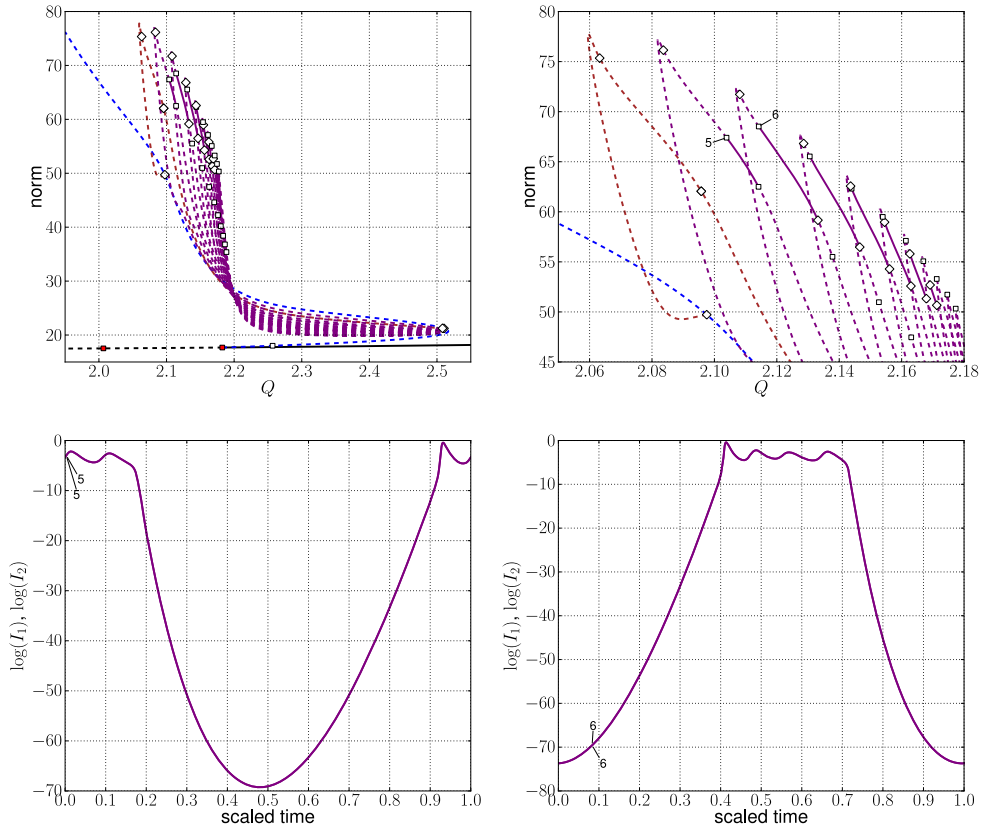

Fig. 3. Top-left: Isolas of in-phase periodic orbits (purple), shown together with the stationary family (black), the in-phase family (blue), and its period-doubled family (brown). Top-right: A blow-up of the top-left panel. Bottom: Representative solutions from the upper panels, namely, solutions along the isolas I_{03} and I_{04}. Coupling parameter $c = 0.14$.

period-doubling bifurcations along the isolas, as the coupling strength c changes. The loci of period-doubling bifurcations remain close to the loci of folds. Most of these can be continued to very small c; in fact, the continuation was stopped at $c = 0.0010$. However, none of the branch points persist until small c. Indeed, as as seen in Fig. 5, each locus of branch points encounters a fold with respect to c. When they exist, namely for larger values of c, there is a region of stable periodic solutions on the corresponding isola; see, for example, Fig. 3. The principal observation is that these regions of stability along the isolas disappear as c becomes smaller.

Laboratory experiments [12–14] show that chaos synchronization of the characteristic PQS pulses is possible for moderate coupling. Our analysis predicts this typically happens for values of the pump (Q) larger than the Hopf bifurcation (HB) of the anti-phase family, and smaller than the HB of the in-phase family; where both HBs are on the nontrivial stationary family. Figure 6 confirms this for $c = 0.14$. Panel (a) shows a time series for $\log(I_1)$ where intermittency can be identified. Panel (b) shows complete synchronization between the coupled lasers when $c = 0.14$. Finally, the histogram in panel (c) shows the probability for the neighborhoods of the UPOs on the in-phase isolas to be visited by the trajectory. This is in agreement with the presence

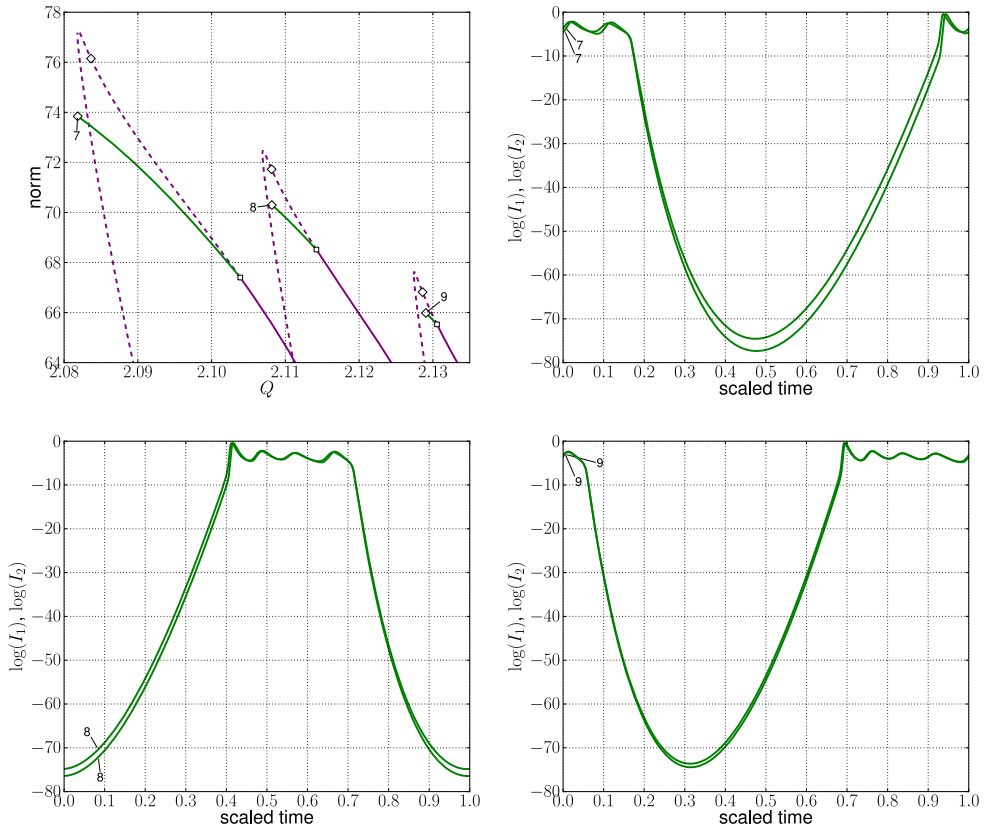

Fig. 4. The top-left panel shows a portion of the isolas I_{03}, I_{04}, and I_{05} (purple), as well as a portion of bifurcating families (green). The other panels show representative solutions along these bifurcating families. Coupling parameter $c = 0.14$.

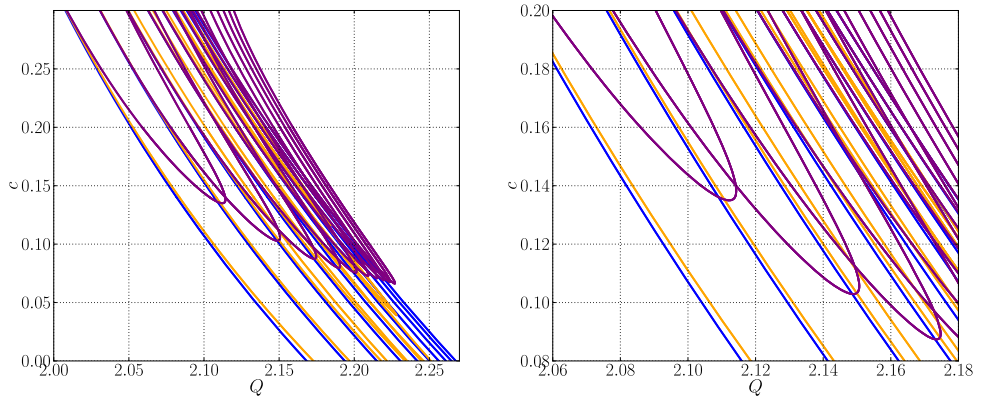

Fig. 5. Loci of folds (blue), period-doubling bifurcations (orange), and loci of branch points (purple) along the isolas I_3 through I_{12}, as dependent on Q and the coupling parameter c. The regions of stability disappear as c becomes smaller, namely at the folds with respect to c along the purple curves.

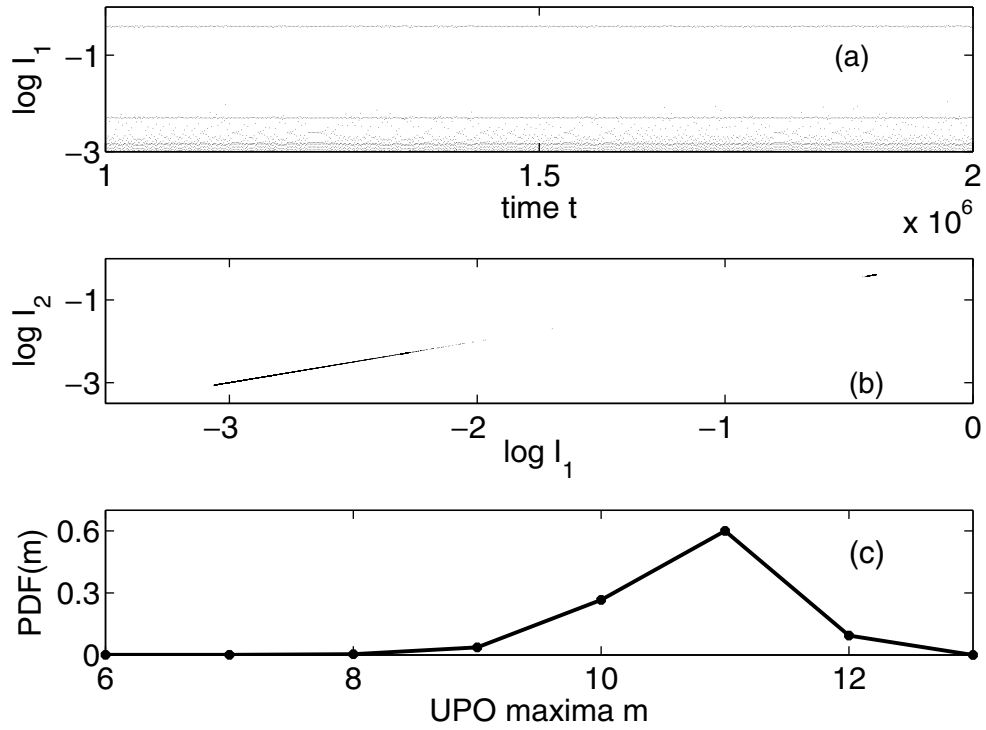

Fig. 6. (a) Time series for $\log(I_1)$. (b) Complete synchronization between the laser oscillators: $\log(I_1)$ versus $\log(I_2)$. (c) Histogram for the number of maxima m characterizing the neighborhoods of visited UPOs (see text). Coupling parameter $c = 0.14$.

of these UPOs in the bifurcation diagram for the pump Q in the top-right panel of Fig. 3. Thus the UPOs of the in-phase isolas constitute the skeleton of the attractor when chaotic synchronization of PQS sets in.

4 Conclusions and discussion

In this article we presented a bifurcation analysis for a model of two coupled CO_2 lasers with a saturable absorber (LSA). The model for each uncoupled laser device displays mixed-mode oscillations with one fast variable and two slow variables, and the phenomenon of period adding cascades. The model for symmetric laser devices includes nonlinear coupling via fast saturable absorbers. In the bifurcation diagrams we show the onset, transition and multistability of in-phase, anti-phase and intermediate-phase oscillations of the system. Relevant new families of periodic orbits are organized along isolas of in-phase, passive Q-switching pulses (PQS). Such isolas have not been observed in a more basic model of coupled lasers with saturable absorbers [17]. As observed in numerical simulations and the bifurcation analysis multistability between new different types of periodic orbits (resonances) and chaotic solutions is a typical feature for moderate coupling strength, where chaotic synchronization may occur. We find that the unstable periodic orbits belonging to the in-phase isolas constitute the skeleton of the attractor when chaotic synchronization of PQS sets in.

This work was supported by NSERC (Canada), BUAP and CONACYT (México).

References

1. M. Brons, T.J. Kaper, H.G. Rotstein, Chaos **18**, 015101 (2008)
2. M. Desroches, J. Guckenheimer, B. Krauskopf, Ch. Kuehn, H.M. Osinga, M. Wechselberger, SIAM Review **54**, 211 (2012)
3. J. Guckenheimer, C. Scheper, SIAM J. Appl. Dyn. Syst. **10**, 92 (2011)
4. J.G. Freire, J.A.C. Gallas, Phys. Lett. A **375**, 1097 (2011)
5. N. Baba, K. Krisher, Chaos **18**, 015103 (2008)
6. M. Desroches, B. Krauskopf, H.M. Osinga, Chaos **18**, 015107 (2008)
7. N.B. Abraham, P. Mandel, L.M. Narducci, *Progress in Optics XXV*, edited by E. Wolf, (North-Holland, Amsterdam,1988), p. 1
8. T. Erneux, P. Glorieux, *Laser Dynamics* (Cambridge University Press, New York, 2010)
9. P. Mandel, *Theoretical Problems in Cavity Nonlinear Optics* (Cambridge University Press, New York, 2005)
10. U. Keller, Nature **424**, 831 (2003)
11. A. Penzkofer, Appl. Phys. B: Photophys. Laser Chem. **46**, 43 (1988)
12. A. Barsella, C. Lepers, D. Dangoisse, P. Glorieux, T. Erneux, Opt. Commun. **165**, 251 (1999)
13. T. Sugawara, M. Tachikawa, T. Tsukamoto, T. Shimizu, Phys. Rev. Lett. **72**, 3502 (1994)
14. I. Susa, T. Erneux, A. Barsella, C. Lepers, D. Dangoisse, P. Glorieux, Phys. Rev. A **63**, 013815 (2000)
15. S. Jalil, I. Belykh, A. Shilnikov, Phys. Rev. E **85**, 036214 (2012)
16. E.M. Izhikevich, *Dynamical Systems in Neuroscience: The Geometry of Excitability and Bursting* (MIT Press, Cambridge, MA, 2007)
17. E.J. Doedel, B. Krauskopf, C.L. Pando, Eur. Phys. J. Special Topics **223**, 2847 (2014)
18. E.J. Doedel, B.E. Oldeman, et al., *AUTO-07P: Continuation and Bifurcation Software for Ordinary Differential Equations* (Concordia University, Montréal, 2011)
19. E.J. Doedel, B.E. Oldeman, C.L. Pando, IJBC **21**, 305 (2011)
20. E.J. Doedel, C.L. Pando, IJBC **22**, 1250238 (2012)
21. J. Dupré, F. Meyer, C. Meyer, Rev. Phys. Appl. (Paris) **10**, 285 (1975)
22. E. Arimondo, F. Casagrande, L. Lugiato, P. Glorieux, Appl. Phys. B: Photophys. Laser Chem. **30**, 57 (1983)
23. M. Tachikawa, K. Tanii, M. Kajita, T. Shimizu, Appl. Phys. B: Photophys. Laser Chem. **39**, 83 (1986)
24. M. Tachikawa, K. Tanii, T. Shimizu, J. Opt. Soc. Am. B **4**, 387 (1987)
25. M. Tachikawa, F.L. Hong, K. Tanii, T. Shimizu, Phys. Rev. Lett. **60**, 2266 (1988)
26. M. Tachikawa, K. Tanii, T. Shimizu, J. Opt. Soc. Am. B **5**, 1077 (1988)
27. D. Hennequin, F. de Tomasi, B. Zambon, E. Arimondo, Phys. Rev. A **37**, 2243 (1988)
28. D. Dangoisse, A. Bekkali, F. Pappof, P. Glorieux, Europhys. Lett. **6**, 335 (1988)
29. M. Lefranc, D. Hennequin, D. Dangoisse, J. Opt. Soc. Am. B **8**, 239 (1991)
30. V.V. Nevdakh, O.L. Gaiko, L.N. Orlov, Opt. Commun. **127**, 303 (1996)
31. L. de B. Oliveira-Neto, G.J.F.T. da Silva, A.Z. Khoury, J.R. Rios-Leite, Phys. Rev. A **54**, 3405 (1996)
32. P.C. de Oliveira, M.B. Danailov, Y. Liu, J.R. Rios-Leite, Phys. Rev. A **55**, 2463 (1997)
33. H.L.D. de S. Cavalcante, J.R. Rios Leite, Chaos **18**, 023107 (2008)